

ACOUSTICAL SEMI-BLIND SOURCE SEPARATION FOR MACHINE MONITORING

Mirko Knaak, Dieter Filbert

Technical University Berlin,
Measurement Technology Lab, Einsteinufer 19, 10587 Berlin, Germany

ABSTRACT

In this contribution, convolutive blind source separation algorithms are compared with the well studied theory of minimum variance beamforming. As a result, the equivalence between the delay vector in the PCA (principle component analysis) subspace and the column of the rotation matrix belonging to the target sound is shown. That equivalence yields a new semi-blind algorithm being more robust than a minimum variance beamformer. The new algorithm is applied to the reconstruction of machine sounds (for classification purposes) when they are corrupted by strong interfering sources and a high noise level in a shop floor.

1. INTRODUCTION

Machine faults modify the machine sound characteristically, therefore observing the machine sound can be a useful mean for fault diagnosis and classification. In a production environment, however, this machine sound is usually corrupted by other interfering sources and non-directive noise, which is often much louder. Negative SNR (Signal-to-Noise-Ratios) occur frequently. The number of sources is not known in advance. All this makes the enhancement of the machine sound a challenging application for blind source separation (BSS). Since most of "true" blind algorithms failed up to our experiments, this semi-blind approach combines blind source separation and minimum variance beamforming (MVB).

Blind source separation deals with the problem of recovering several sources from their linear mixtures. No knowledge about the mixture, i.e. time delay or geometrical relation of sources and microphones is applied. The sources only need to be statistically independent. Signals of different physical sources satisfy this condition.

BSS algorithms can be applied to enhance the machine sound considering the sound of the machine under test (d.u.t. sound) and the (unwanted) interfering sources to be a set of sources. Unlike most applications trying to recover all sources, the recovery of one source is sufficient here. The sound of a rotating machine is periodically (or at least first order cyclostationary) and therefore stationary. The typical

interfering sources are normally not stationary, like human speech, hammer blows or clicking of switches.

Most research is done for BSS with a linear instantaneous mixture model, see [1] and several other approaches in [7]. Due to time-delayed superposition of the sources and reflections from the walls, acoustical mixtures have to be modeled with convolutive mixtures, which have been studied by e.g. [6], [10], [12], [14]. For a comprehensive overview, see [2].

The blind separation of convoluted mixtures (BSCM) implies a separation and deconvolution [2]. The BSCM-algorithms can be distinguished between ICA (independent component analysis) and spatiotemporal BSCM-algorithms [2]. ICA-based algorithms make use of the spatial statistics in the mixtures, in general they need higher than second order statistics to succeed, e.g. [6]. Spatiotemporal algorithms make use of spatial and temporal statistics, e.g. [10].

Most of the approaches have in common that they reduce the problem to instantaneous separation problems for frequency components. The ambiguities left in the recovered frequency components (scaling/ permutation) become a serious problem here. A different permutation of different frequency components leads to mixed outputs and to degraded separation results. Several approaches exist to overcome this problem, e.g. [8], [9], order the output channel according to the maximal correlation between the frequency components or their envelopes [10]. [14] estimates the fourth order cumulants for every frequency component. These algorithms are very time consuming and need much data due to the estimation of the many statistical parameters.

Another problem in this application is determining the number of sources. The method most frequently used when more microphones than sources are present is to separate the signal's subspace into a noise and a signal-plus-noise subspace according to the eigenvalues of the correlation matrix. The background is that the eigenvalues equal to the power of the signals and in the low noise case, the large eigenvalues correspond to the signal and low eigenvalues to the noise. Here, however, the noise's power is in the same range to the d.u.t. signal's power

In contrast to the BSS, non-blind adaptive algorithms, such as the minimum variance beamformer, employ a-priori-

knowledge about the data or the mixture. The MVB needs the direction of propagation of the target signal which is to be estimated. In case of reconstructing the d.u.t. sound, its direction of propagation can be estimated from the geometry of the setup.

Minimum variance beamforming is widely used. Its characteristics and properties is well studied [15]. It belongs to the group of adaptive beamforming (in contrast to the sum-&-delay beamformer used in [16]) shows a good improvement of the SNR as long as the input-SNR is not too weak. Additionally its robustness against estimation errors is limited.

Combining both concepts, BSS and MVB, yields a semi-blind algorithm which tolerates poor estimations of the source location. To derive the algorithm, the following section 2 contains the signal model and an analysis of the beamformer from blind signal processing's point of view. The results are validated with a toy data set. The new algorithm and several tests with toy data and real data are presented in section 3.

2. RELATION BETWEEN MV BEAMFORMING AND BSS

2.1. Signal model

The target sound (d.u.t. sound) s_1 and the interfering coherent sources are considered as one set of sources with $\mathbf{s}_b(t) = [s_{dut}(t), s_{i1}(t) \dots, s_{iM-1}(t)]^T$. Without a loss of generality, the first source is d.u.t. and the others are interfering sources. The sound is measured with an array of N microphones $\mathbf{x}_b(t) = [x_1(t), \dots, x_N(t)]^T$. Due to time delays and reflections from the walls, the microphones receive convoluted mixtures of the sources. This leads to mixing and filtering, since the room acoustics impose a different impulse response a_{mn} between each source s_m and each microphone s_n . Furthermore, incoherent (non-directive) noise is present in a shop floor and regarded as additive noise here (eq. 1).

$$\mathbf{x}_b = \underline{\mathbf{A}} \otimes \mathbf{s}_b + \mathbf{n}_b \quad (1)$$

\otimes is a "matrix convolution" and $\underline{\mathbf{A}}$ contains filter coefficients a_{mn} as elements (instead of scalars):

To employ beamforming algorithms, the broadband wave is decomposed into a superposition of monochromatic waves. Each monochromatic (narrowband) component can be treated independently and formed into the beam signal by applying a phase shift and an attenuation appropriate to the desired delay [15].

$$\mathbf{x}_f = \mathbf{A}_f \cdot \mathbf{s}_f + \mathbf{n}_f \quad (2)$$

In (2), \mathbf{x}_f is a narrowband signal component filtered from \mathbf{x}_b with a band pass centered at f . For the ease of reading, the index f is omitted from here onwards. In case of

an anechoic environment \mathbf{A} consists of the phase shifts and attenuations caused by the time delays τ_{mn} of the sources: $\mathbf{A} = [\mathbf{e}_{a1}, \dots, \mathbf{e}_{aN}]$. \mathbf{e}_{an} is the steering vector of the n^{th} source:

$$\mathbf{e}_{an} = [e^{j2\pi f\tau_{1n}}, \dots, e^{j2\pi f\tau_{Nn}}]^T$$

When multipath mixtures are present, \mathbf{e}_{an} is the sum of the set of paths. \mathbf{e}_{a1} is the delay vector of the d.u.t. sound.

2.2. MV Beamformer

The minimum variance beamformer (BF) uses a coefficient vector \mathbf{w} to reconstruct the d.u.t. sound:

$$y = \hat{s}_1 = \mathbf{w}^H \mathbf{x} \quad (3)$$

To determine \mathbf{w} ; a constrained optimization is applied [15]:

$$\min_{\mathbf{w}} E\{|\mathbf{w}^H \mathbf{x}|^2\} \quad \text{subject to} \quad Re\{\mathbf{w}^H \mathbf{e}_{a1}\} = 1 \quad (4)$$

Eq. (4) minimizes the variance of the beamformer output while preserving the all-pass characteristic in the direction of the d.u.t. sound. Using Lagrange multipliers, eq. (4) can be solved to (5)

$$\mathbf{w} = \frac{\mathbf{R}^{-1} \mathbf{e}_{a1}}{\mathbf{e}_{a1}^H \mathbf{R}^{-1} \mathbf{e}_{a1}} \quad (5)$$

The BF signal reconstruction contains two steps, a projection step ($\mathbf{R}^{-1} \mathbf{e}_{a1}$) and a normalization step ($1/(\mathbf{e}_{a1}^H \mathbf{R}^{-1} \mathbf{e}_{a1})$). Finally, the signal components are combined using a synthesis filter bank to get the broadband signal s_{dut} .

The spatial correlation matrix $\mathbf{R}_x = E\{\mathbf{x} \cdot \mathbf{x}^H\}$ satisfies the model of eq. (6)

$$\mathbf{R}_x = \mathbf{A} \cdot \mathbf{C} \cdot \mathbf{A}^H + \mathbf{K} \quad (6)$$

with \mathbf{C} the coherence matrix between the narrowband source signals

$$\mathbf{C} = \begin{pmatrix} c_{11}|s_{11}|^2 & \dots & c_{1M}s_{1M}s_{M1}^* \\ \vdots & \ddots & \vdots \\ c_{1M}^*s_{1M}^*s_{M1} & \dots & c_{MM}|s_{MM}|^2 \end{pmatrix}$$

and \mathbf{K} the correlation matrix of the incoherent noise components that are assumed to be mutually uncorrelated $\mathbf{K} = \sigma_m \mathbf{I}$.

A precondition for that method is a good estimation of the delay vector \mathbf{e}_{a1} . Therefore, the location of the target sound has to be estimated. Several methods have been proposed for sound localization from measured data [15].

When examining rotating machines, the distances between the d.u.t. and the microphone array are known from the geometry of the experimental setup. Unfortunately, in reverberative environments \mathbf{e}_{a1} does not only correspond to the delay. Furthermore, small errors in the delay estimation lead to a misalignment and therefore to a distortion of the output.

2.3. Coefficient vector in the PCA subspace

Since \mathbf{R}_x is a Hermitian matrix, it has N non zero eigenvalues $\Lambda = \text{diag}[\lambda_1, \dots, \lambda_N]$ and N orthogonal eigenvectors $\mathbf{U} = [\mathbf{e}_{u1}, \dots, \mathbf{e}_{uN}]$ belonging to them. The eigenvalue decomposition of \mathbf{R}^{-1} is

$$\mathbf{R}^{-1} = (\mathbf{U} \cdot \Lambda \cdot \mathbf{U}^H)^{-1} = (\mathbf{U} \cdot \Lambda^{-1} \cdot \mathbf{U}^H)$$

Since the normalization step in (5) does not change the directivity pattern of the beamformer, this section focuses on the projection step. Using the eigenvalue decomposition of \mathbf{R}^{-1} , the projection step of (5) can be rewritten

$$\mathbf{w} = (\mathbf{U} \cdot \Lambda^{-1} \cdot \mathbf{U}^H) \cdot \mathbf{e}_{a1} = \mathbf{U} \cdot \Lambda^{-\frac{1}{2}} \cdot \Lambda^{-\frac{1}{2}} \cdot \mathbf{U}^H \cdot \mathbf{e}_{a1} \quad (7)$$

Defining γ as

$$\gamma = \Lambda^{-\frac{1}{2}} \cdot \mathbf{U}^H \cdot \mathbf{e}_{a1} = \begin{bmatrix} \frac{\mathbf{e}_{u1}}{\lambda_1} \\ \frac{\mathbf{e}_{u2}}{\lambda_2} \end{bmatrix} \cdot \mathbf{e}_{a1} \quad (8)$$

γ_1/γ_2 are the coordinates of \mathbf{e}_{a1} in the subspace spanned by $\frac{\mathbf{e}_{u1}}{\lambda_1}$ and $\frac{\mathbf{e}_{u2}}{\lambda_2}$. With other words, γ is the steering vector transformed by the Karhun-Loeve-Transformation. Finally, rewriting eq. 3 yields (when the normalization step is incorporated into $\tilde{\gamma}$)

$$\hat{\mathbf{s}}_1 = \mathbf{w}^H = \tilde{\gamma}^H \cdot \Lambda^{-\frac{1}{2}} \cdot \mathbf{U}^H \cdot \mathbf{x} \quad (9)$$

2.4. Blind source separation

In contrast to the MV beamforming algorithm (3) where the direction of the d.u.t. signal is used, the blind source separation algorithms do not need any information about the signal or mixing. Furthermore, their goal is to recover all sources.

As stated in (2) the mixing matrix of the narrowband signal component only consists of (complex) scalars. The unmixing matrix \mathbf{W} in (10) will recover these sources:

$$\mathbf{y}(t) = \mathbf{W} \cdot \mathbf{x}(t) \quad (10)$$

Instantaneous BSS/ICA can be employed for every narrowband signal component. Those ICA-algorithms based on order statistics are described in e.q. [1] and those BSS-algorithms based on spatio-temporal statistics in e.g. [13]. They guarantee that $\mathbf{P} = \mathbf{W} \cdot \mathbf{A} = \mathbf{D} \cdot \mathbf{I}$ is a permutation of the unity matrix. The source signals (or their bandpass components) can be recovered up to two ambiguities: permutation and scaling. The estimated source signals are the superposition of the reconstructed bandpass components. A different permutation of different frequency components, therefore, leads to mixed outputs and to degraded separation results. The scaling ambiguity causes distorted outputs.

The main assumption of BSS algorithms is that the source signals are statistically independent. A necessary condition for the independence is $c_{i \neq j} = 0$ in (6). The matrix \mathbf{K} is also assumed to be diagonal.

The estimation of \mathbf{W} consists of two steps: sphering and rotating:

$$\mathbf{W} = \mathbf{T}^H \cdot \mathbf{O} \quad (11)$$

In the first step (sphering), the matrix \mathbf{O} is determined by the principle component analysis (PCA):

$$\mathbf{z} = \Lambda^{-\frac{1}{2}} \cdot \mathbf{U}^H \cdot \mathbf{x} \quad (12)$$

In the second step (rotation) \mathbf{T} a spatio-temporal decorrelation [12],[10] is used. The alternative estimation of \mathbf{T} is the use of higher order statistics e.g. [14].

For statistically independent components, the time-delayed covariance matrices are diagonal, since $\mathbf{R}_s(\tau) = E\{\mathbf{s}(t) \cdot \mathbf{s}^H(t - \tau)\} = \text{diag}[\lambda_{ta_{u1}}, \dots, \lambda_{ta_{uN}}]$ contains the auto-covariances as diagonal elements and the cross-covariances as off-diagonal elements. Therefore, minimizing the off-diagonal elements finally leads to the right correct rotation matrix \mathbf{T} . There are several algorithms solving this constrained optimization problem. The orthogonal matrix \mathbf{T} (the orthogonality is shown in [13]) is determined by a simultaneous diagonalization (with $\mathbf{R}_z(\tau) = \mathbf{O} \cdot \mathbf{R}_x(\tau) \cdot \mathbf{O}^H$).

$$\mathbf{T} = \arg \min_{\mathbf{T}} \sum_{\tau} \sum_{i \neq j} \left| (\mathbf{T} \mathbf{R}_z(\tau) \mathbf{T}^H)_{ij} \right|^2 \quad (13)$$

Integrating eq. 11, 10 and 12 yields:

$$\mathbf{y} = \mathbf{T}^H \cdot \Lambda^{-\frac{1}{2}} \cdot \mathbf{U}^H \cdot \mathbf{x} \quad (14)$$

To reconstruct the broadband d.u.t. signal, the appropriated components of the output vector \mathbf{y} with a proper scaling have to be assembled. Although various methods to overcome the permutation/scaling problem have been presented [9],[8], it is still the main obstacle to that method.

2.5. BSS vs. MV Beamforming

Comparing the eq. (9) and (14) shows the equivalence of the two concepts:

$\tilde{\gamma}$ shares the direction of the column of \mathbf{T} that belongs to the d.u.t. sound.

Or, with $T = (\mathbf{e}_{T1}, \dots, \mathbf{e}_{TN})$

$$\tilde{\gamma} \propto \mathbf{e}_{T_{opt}} \quad (15)$$

With this equivalence, the BSS algorithm can be improved. The knowledge of $\tilde{\gamma}$ helps to choose the right component. Furthermore, it gives some information about the amplitude of the band passed component by the normalized $\tilde{\gamma}$. However, the algorithm is not blind anymore.

The array gain of the beamformer can also be increased. When the estimation of \mathbf{e}_{a1} is not precise, the coefficient vector may be adjusted with \mathbf{T} . Combining both concepts

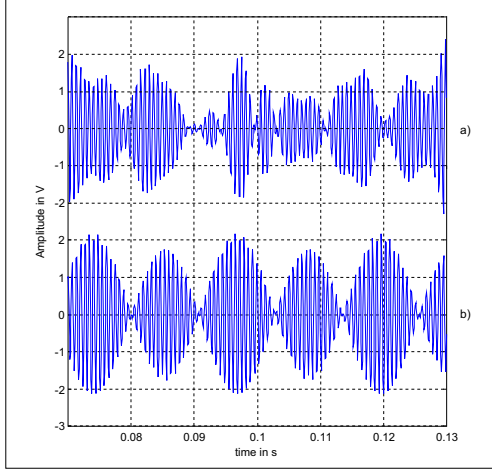


Fig. 1. Band passed source signal: (a) Machine signal,(b) Interfering signal

yields an algorithm that needs prior information but is less sensitive to them.

The equivalence of the two concepts can be demonstrated with a toy data set. Two band passed signals s_1 and s_2 are mixed by a mixing matrix \mathbf{A} . The band pass has a bandwidth of 160 Hz and is centered at 1470 Hz. The sampling rate is 11.025 kHz. Although in reality the source vector \mathbf{s} and the mixing matrix \mathbf{A} are complex valued, real valued data are used for visualization purposes. Fig. 1 shows the demonstration signals.

The signal s_1 is derived from a machine sound of a small d.c. motor. The motor signal is a very broadband signal covering a frequency range from several Hz (rotational frequency $f_0 = 60 - 100\text{Hz}$) to several kHz.

As stated in [11] band passed signal components of electrical motors are modulated by the rotation frequency (fig. 1a). The amplitude modulation can be written as in eq. (16): $\cos(2\pi ft)$ is the carrier signal with the modulation of the rotating frequency $(1 + \cos(2\pi f_0 t))$. Other modulations may occur and are modeled by $u_f(t)$.

$$\Re\{\mathbf{s}(t)\} = \cos(2\pi ft) \cdot u_f(t) \cdot (1 + \cos(2\pi f_0 t)) \quad (16)$$

This periodic modulation distinguishes the motor signal from the interfering sounds. Non-periodic interfering sounds, such as human speech, hammer blows and other noises in a shop floor, do not show periodic modulations. Other rotating machines have a different rotational frequency and therefore a different modulation. s_2 is the band pass signal of a non-periodic signal of the same band pass (fig 1b).

The scatter plot of the mixed signals is shown in fig. 2 with the PCA vectors $\mathbf{e}_{u1}/\mathbf{e}_{u2}$. They point in the directions of the greatest variances, which are not equal to the direction (in the statistical sense) of the sources. The steering vector \mathbf{w} is orthogonal to the interfering component, so

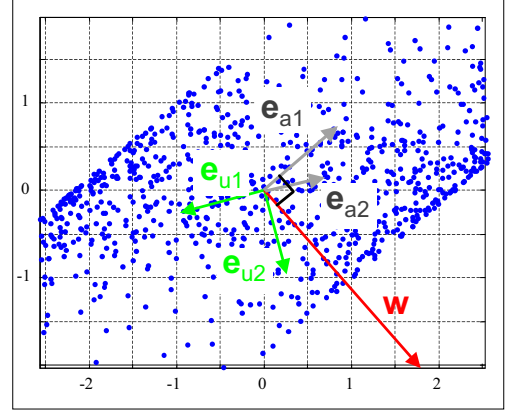


Fig. 2. Scatter plot of the mixed signals with the vectors of the sphering matrix $\mathbf{e}_{u1}/\mathbf{e}_{u2}$ and the coefficient vector \mathbf{w}

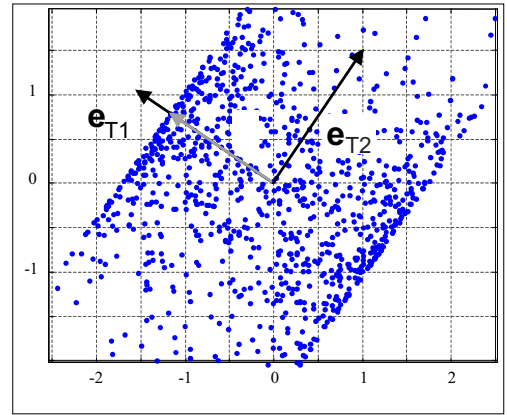


Fig. 3. Scatter plot of the mixed signals in the PCA subspace with the vectors of the rotation matrix $\mathbf{e}_{T1}/\mathbf{e}_{T2}$ and the transformed delay vector \mathbf{w}

that it minimizes the interfering source's contribution to the beamformer's output.

Fig. 3 shows the data in the PCA subspace. γ and \mathbf{e}_{T1} point in the same direction as expected.

3. ALGORITHM AND RESULTS

The principle of the algorithm is already stated in eq. (15). The PCA and the transformation of the delay vector into that subspace in the first step. The second step is to choose the best column of \mathbf{T} (17).

$$\mathbf{e}_{T_{opt}} = \min_{\mathbf{e}_{Tk} \in \mathbf{T}} \angle(\gamma, \mathbf{e}_{Tk}) \quad (17)$$

The third step is to rescale $\mathbf{e}_{T_{opt}}$ (18)

$$\tilde{\mathbf{e}}_{T_{opt}} = \mathbf{e}_{T_{opt}} / (\mathbf{e}_{a1}^H \mathbf{R}^{-1} \mathbf{e}_{a1}) \quad (18)$$

The algorithm is applied to several sets of data. First, the evaluation data from 2.5 with an artificial mixture is used.

	MV	BSS	New Algorithm
τ correctly estimated	19 dB	3 dB	10 dB
τ incorrectly estimated (error 5%)	5 dB	3 dB	8 dB

Table 1. SNR improvement of the semi-blind algorithm

Secondly, the algorithm is applied to real data measured in an office room.

In the evaluation data set, the source data vector is projected to eight "microphones" by a mixing matrix containing short FIR-filters (actually an extension T. W. Lee's testing filters [6] to a 8×2 -matrix.) The delay vector is known by the number of leading sources of the elements in the first column of \underline{A} . It is varied to study the robustness of the algorithms. To remain close to the application, the interfering source (s_2) is five times higher than the d.u.t. sound (s_1). The additive noise is band limited because it is supposed to model the incoherent noise in the production site.

The numerical results are shown in table 1. The signal separation is measured by a frequency dependent signal to noise-ratio as in other publications (e.g. [8]). It is defined by the ratio of the d.u.t. sound's power and the power of the interfering components. When the correct delay vector is utilized, the best results are achieved by the minimum variance beamformer. That is not very surprising because the algorithm exploits the whole available information. When the estimation of the delay vector becomes less reliable the coefficient vector of MV points into a wrong direction. The results of the new combined algorithms are superior. The standard BSS algorithm facing the problems of scaling and permutation yields almost no improvement of the SNR.

The case of an incorrect estimation of the delay vector is illustrated with fig. 4 and fig. 5. The spectrograms in fig. 5 have high time and low frequency resolution so that the periodic intensity modulation of the rotational machine's spectral lines (already stated in 16) become visible in fig. 5a. Their height and strength can be exploited for the extraction of meaningful features. While invisible in the mixed signal 5b, fig. 5c show its successful reconstruction.

The power spectra (fig. 4) have a high spectral resolution. For rotating machines, the spectrum vanishes between the order lines. The spectral parts of the harmonic frequencies are significantly higher. The spectrum is significantly improved, since harmonic frequencies are not dominant in the mixed signal while they do so in the reconstructed signal. Informal hearing tests showed a similarity between the motor signal and the reconstructed signal. The interfering sources almost vanished.

A drawback is that the amplitudes of the harmonics are

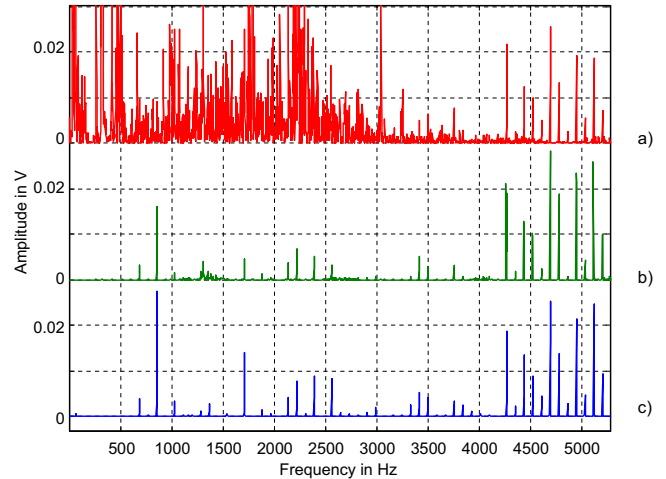


Fig. 4. Power spectra: Mixed (a), and source (c) signal

not perfectly recovered. One reason might be the deployment of the incorrect delay vector in the normalization step of the new algorithm (18)

The results with real world data are shown in fig. 6. The setup was an equally spaced linear microphone array (4 microphones, $\Delta = 400mm$) in a small office room. The target sound was a human voice and recorded music served as the interfering sound. The known delay vector was slightly modified. The figure shows the improvement qualitatively. Unfortunately, we still do not have a quantitative assessment (including the influence of the reflections) or a motor test with real world data.

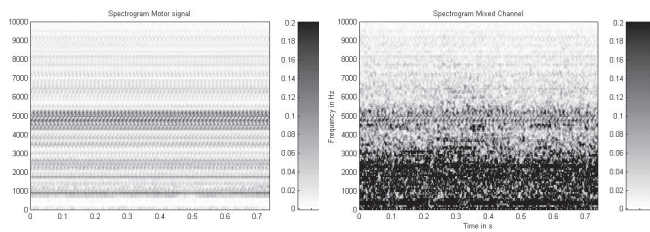
4. SUMMARY

The new approach introduced here is the utilization of a-priori-knowledge for BSS algorithms to reconstruct the sound of rotating machines. This utilization restricts the range of the new method and actually leads to a semi-blind algorithm. Nevertheless, it bears a solution of several problems of BSCM-algorithms: the permutation and the scaling problem as well as the unknown number of sources.

Due to its robustness against unprecise assumptions, the proposed system is applicable to a wide range of classification problems of highly noise-corrupted data. Especially in cases where conventional methods fail, the employment of the new approach as a preprocessor allows improved classification results.

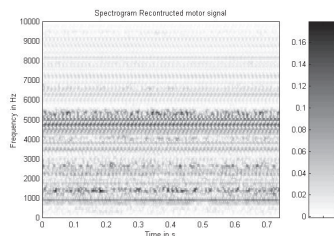
5. REFERENCES

- [1] Anthony Bell, Terence Sejnowski *An information-maximization approach blind source separation and blind deconvolution, Neural Computation, 7, 6, 1004-1034 (1995)*



(a) Motor signal

(b) Input signal



(b) Reconstructed signal

Fig. 5. Spectrograms

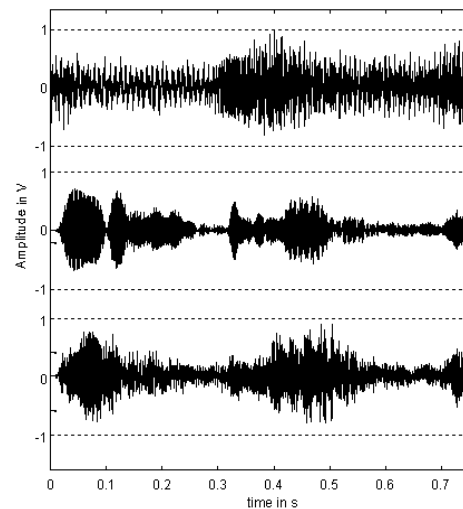


Fig. 6. Reconstruction of real world data: Measured signal a), reconstructed signals with MVB-BSS b) and with MVB c)

- [2] Kari Torkkola *Blind separation of delayed and convolved mixtures*, in *Unsupervised adaptive filtering, Vol. 1: Blind source separation*, Simon Haykin (Ed.), John Wiley, New York, 2000
- [3] P. Fabry, Ch. Serviere, *Blind separation of noisy harmonic signals using orthogonal techniques for rotating machine diagnosis*, *Proc. of 2nd. Int. Workshop of ICA 2000, Helsinki*
- [4] Alexander Ypma, Amir Leshem *Blind separation of machine vibration with bilinear forms*, *Proc. of 2nd. Int. Workshop of ICA, Helsinki, 2000*
- [5] D.W.E. Schobben, P.C.W. Sommen "On the Indeterminacies of Convolutional Blind Signal Separation based on Second Order Statistics," *Int. Symposium on Signal Processing and its Applications (ISSPA), Brisbane, Australia, 1999, 215-218*
- [6] Te-Won Lee, Anthony Bell, Reinhold Orglmeister "Blind Source Separation of Real World Signals," *Int. Conf. Neural Networks, Houston May 97, 1997*
- [7] Simon Haykin (Ed.) *Unsupervised adaptive filtering, Vol. 1: Blind source separation*, John Wiley, New York, 2000
- [8] Jörn Anemüller, Birger Kollmeier *Amplitude modulation for convolutional blind source separation*, *Proc. of 2nd. Int. Workshop of ICA, Helsinki, 2000*
- [9] Hsiao-Chun Wu, Jose C. Principe *Simultaneous Diagonalization in the frequency domain (SDIF) for source separation*, *Proc. Workshop ICA 99, Jan 11-15, Aussois, France, 1999*
- [10] S. Murrata, S. Ikeda, A. Ziehe *An approach to blind source to blind source separation based on temporal structure of speech signals*, *BSIS, Technical report, Nr. 2, 1998* <http://www.bsp.brain.riken.go.jp>
- [11] M.Knaak, M. Fausten, D. Filbert *Acoustical machine monitoring using blind source separation*, *4th Proc. of Int. Conf. on acoustical and vibratory surveillance methods and diagnostics techniques Compiègne, France, Sept. 2001, (excepted)*
- [12] F. Asano, Y. Motomura, H. Asoh T. Matsui *Effect of PCA filter in blind source separation*, *Proc. of 2nd. Int. Workshop of ICA, Helsinki, 2000*
- [13] A. Belouchrani, K. Aded-Meraim, J. Cardoso, *A blind separation technique using second order statistics*, *IEEE Transactions on signal processing, 45 (2), 434-444, 1997*
- [14] Cristina Mejuto, Adriana Dapena, Luis Castedo *Frequency-domain infomax for blind separation of convolutional mixtures*, *Proc. of 2nd. Int. Workshop of ICA, Helsinki, 2000*
- [15] D. H. Johnson, D. E. Dudgeon *Array signal processing*, Prentice Hall, Englewood Cliffs, 1993
- [16] Jean-Francois Cardoso, Antoine Souloumiac *Blind Beamforming for non gaussian signals*, *IEE Proceedings, vol. 140, no. 6, pp. 362-370, 1993*